Effects of nickel-loading method on the water-splitting activity of a layered $NiO_x/Sr_4Ti_3O_{10}$ photocatalyst

Young-Gwan Ko and Wha Young Lee *

School of Chemical Engineering, Seoul National University, Shinlim-dong San 56-1, Kwanak-ku, Seoul, 151-742, Korea

Received 2 April 2002; accepted 19 June 2002

$Sr_4Ti_3O_{10}$, which is known to have a Ruddlesden-Popper phase as a layered perovskite-type oxide, showed activity leading to the decomposition of pure water into H_2 and O_2 without any co-catalyst, when irradiated with light under 395 nm. When NiO_x was loaded onto $Sr_4Ti_3O_{10,}$ both by the impregnation (I) method and the vapor deposition (VD) method, this photocatalytic activity drastically increased. Nickel acetylacetonate, when used with the VD method, was found to give rise to more efficient photocatalytic activity than that obtained using nickel nitrate with the impregnation method.

KEY WORDS: photocatalyst; $Sr_4Ti_3O_{10}$; water decomposition; H_2 evolution; nickel acetylacetonate; vapor deposition method.

1. Introduction

Hydrogen is currently produced from fossil fuels on an industrial scale. However, much attention has been focused on the direct splitting of water for H_2 generation. Since the report of Fujishima and Honda in 1971 [1], the photocatalytic decomposition of water using several semiconducting oxides, such as TiO_2 [2], $SrTiO_3$ [3], $K_4Nb_6O_{17}$ [4], $BaTi_4O_9$ [5] and $NaTaO_3$ [6], has been studied. The main structure of these catalysts consists of a 4A element (Ti) and a 5A element (Nb, Ta). $K_4Nb_6O_{17}$ and $NaTaO_3$ exhibit water-splitting activity without any co-catalyst or additive. Among the common loading metals, *i.e.*, Ni, Ru, Pt, Pd, the best activity is usually obtained from Ni and Ru.

In this study, $Sr_4Ti_3O_{10}$, a layered perovskite-type oxide was prepared using a polymerized complex method, which is a variant of the sol-gel method. $Sr_4Ti_3O_{10}$ is reported to exhibit overall water-splitting photocatalytic activity without any co-catalyst, and, in this study, a new efficient precursor (nickel acetylacetonate) and method (vapor deposition, VD) to load nickel onto the photocatalyst is investigated.

2. Experimental procedures

$Sr_4Ti_3O_{10}$ was prepared by both the solid-state reaction method (SSRM) and the polymerized complex method (PCM) in order to compare the resultant activity. When using the SSRM method, $SrCO_3$ and TiO_2 were mixed in stoichiometric proportions, calcined at 1100 °C for 30 h, and intermittently pelletized during calcination. In the case of the PCM method, $Ti(O\textit{i}Pr)_4$ was added to an ethylene glycol and methanol mixture, then citric acid and $Sr(NO_3)_2$ were added to the solution in this order, resulting in a one-phase transparent solution. After polyesterification at 130 °C for over 20 h, a polymerized complex gel could be made. There was no formation of visible precipitation during gelation. $Sr_4Ti_3O_{10}$ was finally synthesized by heating the precursor at 800–1100 °C for 2 h. The $Sr_4Ti_3O_{10}$ powder was washed with distilled water to eliminate the residue. Nickel was loaded by the impregnation method either with an aqueous solution of $Ni(NO_3)_2$ or with $Ni(C_5H_7O_2)_2$, which is equivalent to $Ni(acac)_2$, in acetone followed by drying at 80 °C overnight. Nickel was also loaded by the VD method using $Ni(acac)_2$ at 233 °C for 2 h in N_2. The nickel-loaded $Sr_4Ti_3O_{10}$ powder was calcined at 300 °C for 1 h in air. H_2 reduction was performed at 500 °C for 2 h and then O_2 reoxidation at 200 °C for 1 h.

The prepared powder structures were characterized by X-ray diffraction (XRD, Rigaku, D/MAX-IIA). Surface area was determined by BET measurement (Micromeritics, ASAP 2010). A diffuse reflection spectrum was obtained by UV-DRS (Perkin Elmer, Lambda 20) and was converted from reflection to absorbance by the Kubelka-Munk method. The amount of loaded Ni was determined by ICP (VG elemental Ltd., VG PQ2-Turbo). Ni particle size was determined by TEM (JEOL, JEM-200CX). The state of loaded Ni was investigated by XPS (VSW, ARIESARSC 10MSD).

The photocatalytic reaction was carried out in an air-free closed gas circulation system with an inner irradiation cell made of quartz (345 cm^3). The catalyst (1 g) was dispersed in distilled water (475 cm^3) by magnetic

---

* To whom correspondence should be addressed.
E-mail: wyl@snu.ac.kr

1011-372X/02/1100-0157/0 © 2002 Plenum Publishing Corporation

stirring and was irradiated using a high-pressure Hg lamp (Young Kwang Corporation, 400W) under an Ar atmosphere. The amount of evolved gases was determined by gas chromatography (Chrompack, MS-5A, TCD, Ar carrier).

3. Results and discussion

We investigated $Sr_4Ti_3O_{10}$ for the photocatalytic decomposition of water, which crystallizes with triple layers of TiO_6 octahedra in the stack and has a neutral interlayer with high electron density. It is normally used as a material in solid oxide fuel cells (SOFC), exhibiting a high degree of flexibility in manipulating the electrical and transport properties of ionic solids, and is assumed to have properties beneficial to photoactivity. Figure 1 shows the XRD patterns of the synthesized $Sr_4Ti_3O_{10}$, which were identical to the one previously reported [7]. A (107) phase is observed at about 32°, which indicates a layer consisting of three TiO_6 octahedra in height, which was observed to grow as the calcination temperature increased. When the oxide was prepared by PCM, a temperature of over 700 °C was required to form the desired structure, and the oxide calcined at 900 °C showed the highest activity for water photodecomposition. But a temperature of over 1100 °C was required to get the exact structure when the oxide was prepared by SSRM. This is due to impurities resulting from the difficulty of interdiffusion of the precursors during calcination. The XRD pattern of $Sr_4Ti_3O_{10}$ observed before the reaction was identical to that measured after a prolonged reaction (20 h), and consistent activity pattern was also observed, suggesting that the catalyst is stable under UV light and in the aqueous medium.

BET surface area measured by N_2 adsorption at 77 K was 8.51–4.96 m^2/g for PCM and 3.49 m^2/g for SSRM respectively. The higher surface area obtained from PCM than from SSRM can be attributed to a lower calcination temperature and to the superiority of the former method.

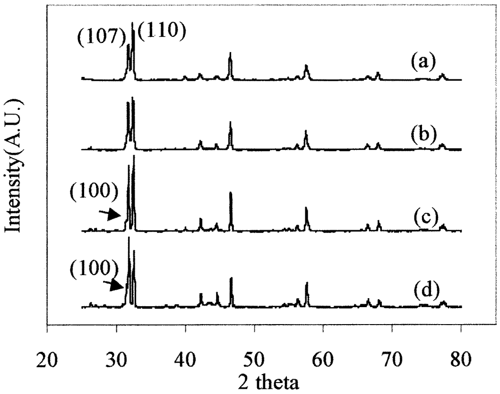

Figure 1. XRD patterns of $Sr_4Ti_3O_{10}$ calcined at (a) 800 °C, (b) 900 °C, (c) 1000 °C for 2 h by PCM, and calcined at (d) 1100 °C for 30 h by SSRM.

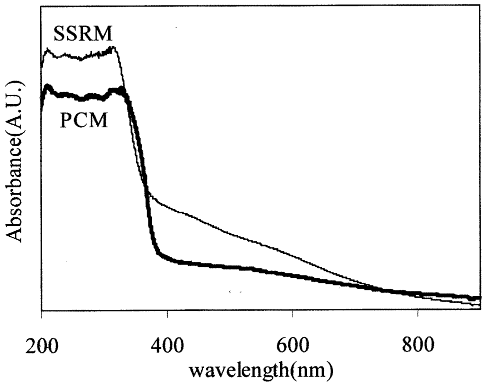

Figure 2. UV-DRS of $Sr_4Ti_3O_{10}$.

The light absorption band was measured to be under 395 nm by UV-DRS (figure 2). The band gap of the catalyst, 3.2 eV, can be estimated from plots of the square root of Kubelka-Munk functions F(R) *versus* photon energy. The sleeve observed at the band edge for $Sr_4Ti_3O_{10}$ (SSRM) is assumed to be due to the presence of impurities, which is confirmed by the resultant low photocatalytic activity.

The smaller particle size of $K_4Nb_6O_{17}$ reportedly enhances water-splitting activity [8]. Therefore, we investigated if the particle size of nickel loaded using a new loading method also significantly affects the photocatalytic activity required for water splitting. Inoue *et al.* [9] reported that $Ru_3(CO)_{12}$ formed smaller RuO_2 particles and gave a larger number of active sites than $RuCl_3$ as a precursor for Ru impregnation on $BaTi_4O_9$. Similarly, $Ni(acac)_2$ is assumed to have the capability of giving a more uniform distribution with smaller nickel particles, thus giving rise to a larger number of active sites than when using $Ni(NO_3)_2$ as a precursor for Ni loading onto $Sr_4Ti_3O_{10}$. Also, vapor deposition (VD) at a temperature slightly higher than sublimation temperature, 228 °C, gave rise to a better dispersion degree, when compared to impregnation (I) of $Ni(acac)_2$ in acetone onto the $Sr_4Ti_3O_{10}$.

The effect of the amount of nickel and nickel precursor and loading method on photocatalytic activity, resulting in water decomposition over $Sr_4Ti_3O_{10}$, is shown in figure 3. The non-loaded $Sr_4Ti_3O_{10}$ alone is active (0.7 μmol/h), but activity was enhanced by nickel loading. The highest activity (H_2 evolution rate of 170 μmol/h) was achieved when 2.7 wt% of Ni was loaded by VD using $Ni(acac)_2$ on $Sr_4Ti_3O_{10}$ prepared by PCM. The quantum yield, defined as the number of electrons and holes consumed for H_2O_2 evolution of $Sr_4Ti_3O_{10}$ per that of incident photons, was estimated to be *ca* 4.5% at 360 nm. For $Sr_4Ti_3O_{10}$ prepared by SSRM, 5 wt% nickel-loaded $Sr_4Ti_3O_{10}$ showed the highest activity. However, activity varied according to the $Sr_4Ti_3O_{10}$ preparation method. Good results were

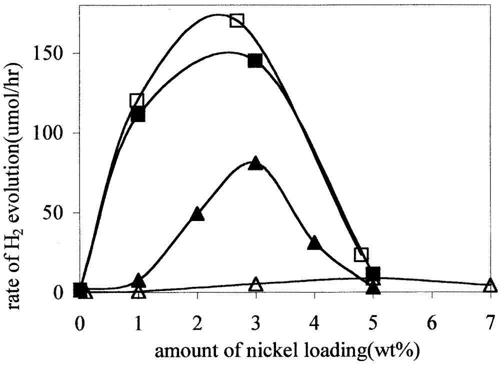

Figure 3. Activity dependence of $Sr_4Ti_3O_{10}$ upon the amount of nickel loading. □ $Ni(acac)_2$-CVD/$Sr_4Ti_3O_{10}$(PCM); ■ $Ni(acac)_2$-I/$Sr_4Ti_3O_{10}$ (PCM); ▲ $Ni(NO_3)_2$-I/$Sr_4Ti_3O_{10}$ (PCM); △ $Ni(NO_3)_2$-I/$Sr_4Ti_3O_{10}$(SSRM).

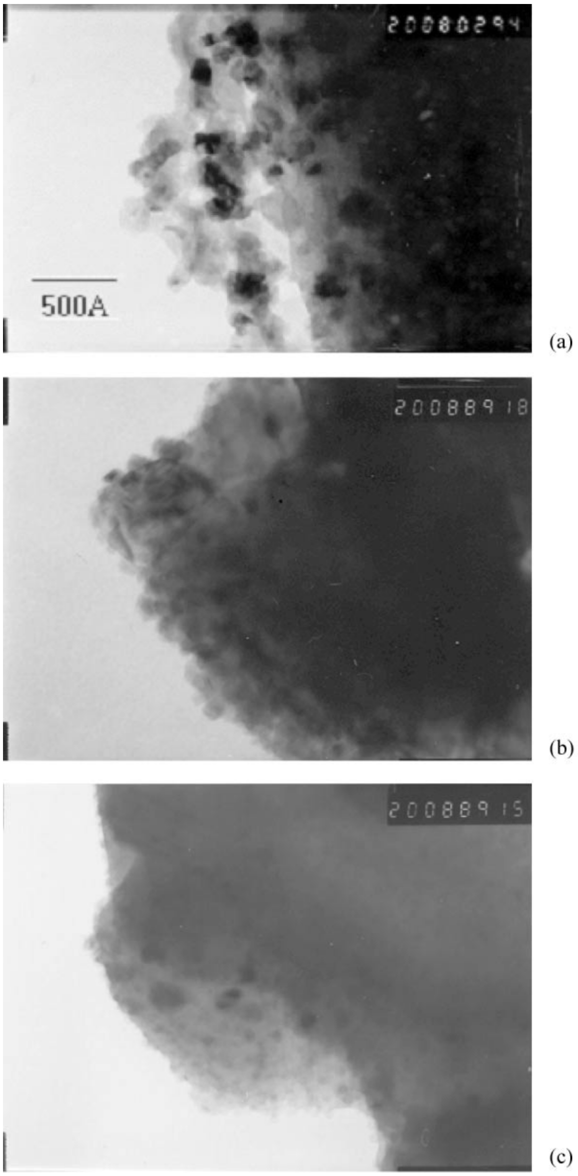

Figure 4. TEM image of $NiO_x/Sr_4Ti_3O_{10}$ (PCM) catalysts (×200 000). (a) 3 wt% $Ni(NO_3)_2$-I; (b) 3 wt% $Ni(acac)_2$-I; (c) 2.7 wt% $Ni(acac)_2$-VD.

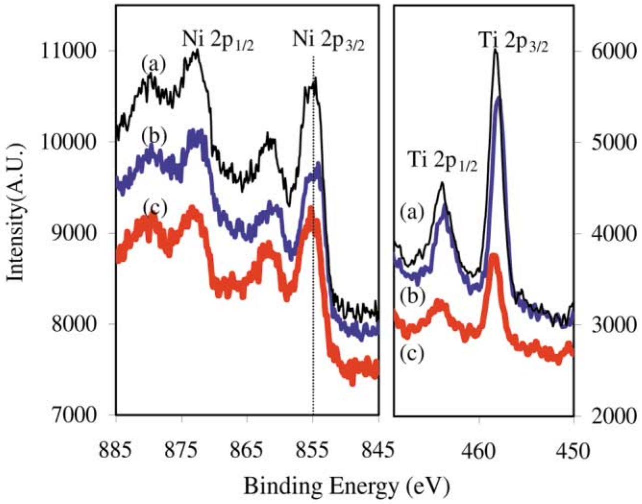

Figure 5. XPS spectra of $NiO_x/Sr_4Ti_3O_{10}$ (PCM) catalysts. (a) 3 wt% $Ni(NO_3)_2$-I; (b) 3 wt% $Ni(acac)_2$-I; (c) 2.7 wt% $Ni(acac)_2$-VD.

obtained using the PCM method. PCM may provide a relatively uniform morphology and homogeneity of $Sr_4Ti_3O_{10}$, so that activity degradation by impurities could be reduced. When $Ni(acac)_2$ is utilized as a nickel-loading precursor, photocatalytic activity is enhanced. The gas formation rate over the $Ni(acac)_2$-derived $NiO_x/Sr_4Ti_3O_{10}$ catalyst is almost twice as much as that over the $Ni(NO_3)_2$-derived $NiO_x/Sr_4Ti_3O_{10}$. This is probably due to the fact that $Ni(acac)_2$ is more bulky than $Ni(NO_3)_2$, resulting in the formation of small nickel particles.

The particle size of loaded nickel was measured to be *ca* 25 nm, 15 nm, and 10 nm on average, respectively, from the TEM images shown in figure 4. The surface state of the catalysts was determined by XPS (figure 5), and the results are summarized in table 1. $Ni(acac)_2$ prepared by the VD method showed *ca* 40% higher Ni dispersity and stronger Ni binding energy than that prepared by the impregnation method. This means that loaded Ni particle by the VD method makes a stronger bond with the surface of $Sr_4Ti_3O_{10}$, and thus there could be smaller agglomeration during the following preparation steps at higher temperature, *i.e.*, calcination and reduction. The slight difference in photoactivity according to loading method found for $Ni(acac)_2$ may be due to differences in the nickel-loaded site. In the VD method, nickel deposition is assumed to be formed

Table 1
XPS peak intensity ratio of Ni $2p_{3/2}$/Ti $2p_{3/2}$ and binding energy.

$NiO_x/Sr_4Ti_3O_{10}$ (PCM)	I(Ni $2p_{3/2}$/Ti $2p_{3/2}$)	Ni $2p_{3/2}$ (eV)	Ti $2p_{3/2}$ (eV)
3 wt% $Ni(NO_3)_2$-I	1.7781	854.6	458.3
3 wt% $Ni(acac)_2$-I	1.7784	854.1	457.9
2.7 wt% $Ni(acac)_2$-VD	2.4638	855.3	458.5

either by thermal deposition onto previously deposited $Ni(acac)_2$ and by coordination through a donor interaction between the surface oxygen and the metal center [10] or by reaction of the $Ni(acac)_2$ with the surface hydroxyl groups of the support, as follows [11]:

$$\mathrm{M{-}OH} + \mathrm{Ni(acac)_2} \rightarrow \mathrm{M{-}O{-}Ni{-}(acac)} + \mathrm{H(acac)}.$$

Presently, it is not a simple task to conclude which is the dominant mechanism. However, XPS results show that simple thermal deposition, which is rather weak binding, is not the dominant one. Nonetheless, the VD method would be a reasonable explanation for the more strongly bonded Ni particle to the surface of $Sr_4Ti_3O_{10}$ than simply impregnated Ni particle, as inferred from the binding energy in the XPS result.

It is concluded that $Ni(acac)_2$ leads to smaller nickel particles due to its bulky property than $Ni(NO_3)_2$. The vapor deposition method leads to smaller agglomeration than the impregnation method, because loaded nickel particle in the vapor deposition method binds more strongly with the surface of $Sr_4Ti_3O_{10}$ than in the impregnation method. These two factors result in the enhanced activity for photocatalytic water splitting.

Acknowledgment

This work was supported by the Korea Energy Management Corporation (KEMCO), Korea.

References

[1] A. Fujishima and K. Honda, Bull. Chem. Soc. Jpn. 44 (1971) 1148.

[2] K. Yamaguchi and S. Sato, J. Chem. Soc. Faraday Trans. I 81 (1985) 1237.

[3] J.M. Lehn, J.P. Sauvage, R. Ziessel and L. Hilaire, Israel J. Chem. 22 (1982) 168.

[4] A. Kudo, A. Tanaka, K. Domen, K. Maruya, K. Aika and T. Onishi, J. Catal. 111 (1988) 67.

[5] Y. Inoue, T. Kubokawa and K. Sato, J. Chem. Soc. Chem. Commun. (1990) 1298.

[6] H. Kato and A. Kudo, Catal. Lett. 58 (1999) 153.

[7] G.J. McCarthy, W.B. White and R. Roy, J. Am. Ceram. Soc. 52 (1969) 463.

[8] S. Ikeda, A. Tanaka, K. Shinohara, M. Hara, J.N. Kondo, K. Maruya and K. Domen, Microporous Materials 9 (1997) 253.

[9] S. Ogura, M. Kohno, K. Sato and Y. Inoue, J. Mater. Chem. 8(11) (1998) 2335.

[10] J.C. Kenvin, M.G. White and M.B. Mitchell, Langmuir 7 (1991) 1198.

[11] M. Lindbald, L.P. Lindfors and T. Suntola, Appl. Surf. Sci. 75 (1994) 220.